Zeitschrift: Helvetica Physica Acta
Band: 65 (1992)
Heft: 2-3

Artikel: Surface acoustic wave studies of the fractional quantum Hall regime
Autor: Willet, R.L. / Paalanen, M.A. / Pfeiffer, L.N.
DOI: https://doi.org/10.5169/seals-116393

Surface Acoustic Wave Studies of the Fractional Quantum Hall Regime

R. L. Willett, M. A. Paalanen, L. N. Pfeiffer, K. W. West, R. R. Ruel

AT&T Bell Laboratories
600 Mountain Avenue
Murray Hill, N.J. 07974 U.S.A.

Abstract. Surface acoustic wave (SAW) propagation on high quality AlGaAs/GaAs heterostructures is examined in the fractional quantum Hall regime. By measuring the transmitted SAW amplitude and frequency the 2D electron system (2DES) conductivity at the SAW frequency can be deduced and compared to the measured d.c. conductivity. Up to about 500MHz the SAW derived conductivity does not differ substantially from the measured d.c. conductivity. At higher frequencies some deviations are observed at FQHE and IQHE states. However, at Landau level filling $\nu = 1/2$ SAW propagation is markedly different from that observed in the neighboring filling factor range; the response to the SAW is the opposite of that suggested by the d.c. conductivity. In addition, anomalous sound propagation is also observed in the small filling factor range $\nu \lesssim 1/5$, where electron solid formation is suspected. The properties of these distinct SAW anomalies are described and their possible origins discussed.

The purpose of our experiments is to study the response of a correlated 2D electron system to a time and spatially varying electric field. Electron correlations are present in the extreme quantum limit of low disorder 2DES: the fractional quantum Hall effect[1] occurs at odd denominator fillings factors and at higher magnetic fields electron solidification[2] is proposed. The technique we employ is similar to that used by Wixforth et. al.[3] in which a surface acoustic wave is propagated on a GaAs/AlGaAs heterostructure. The 2DES interacts with the piezoelectric field of the SAW, affecting the sound amplitude and velocity and allowing inference of the frequency and wave-vector dependent conductivity from the SAW properties. We have used multiple SAW transducers each producing several harmonics so that a wide range of ω and k can be examined. Direct comparison is then made with simultaneously measured d.c. transport.

At low SAW frequencies (<500MHz) the electron response can be modeled using the d.c. sheet conductivity. This modeling breaks down at high frequencies in three distinctive filling factors regimes: at $\nu = 1/2$, the center of the lower spin split Landau level; at FQHE and IQHE states for our highest SAW frequencies; and at $\nu \lesssim 1/5$ where electron solid formation has been suggested. These findings of anomalous sound propagation will be the focus of our study.

FQHE and IQHE

We have examined a total of 10 high quality GaAs/AlGaAs single interface heterostructures with areal electron densities $< 2 \times 10^{11}$ cm^{-2} and with high mobilities ranging from $\sim 1-4 \times 10^6$ cm^2/V$-$sec. Each sample was grown with typically 5000 Å between the sample surface and the 2DES, which is considerably less than the shortest SAW wavelength of 2μm: the SAW penetrates only about one wavelength from the surface. The cap layer, dopant layer, spacer and 2D gas region were etched on either end of the samples leaving

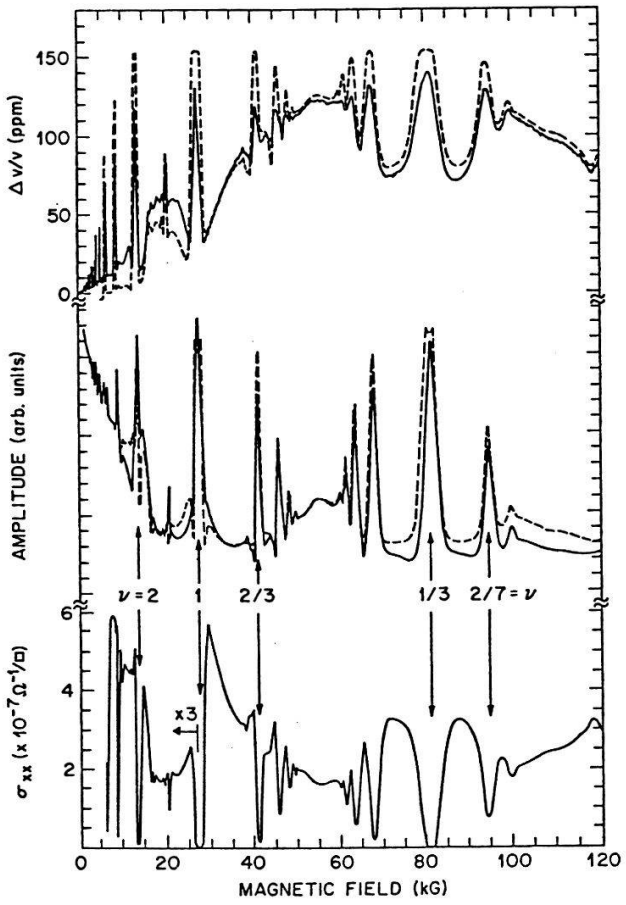

Figure 1. Conductivity, surface acoustic wave amplitude and velocity shift versus magnetic field at 160 mK and 235 MHz in sample #1. Solid lines are measured values, dashed lines are results of the conductivity model using the measured σ_{xx} (B) and $\sigma_m = 4 \times 10^{-7}\Omega^{-1}$.

2DES free zones where SAW transducers were patterned. The rectangular mesa remaining between the transducers provided a 2DES path of >1 mm. Indium contacts were diffused into the periphery of the 2DES mesa to allow transport measurement using standard lock-in techniques. The interdigital SAW transducers were patterned using electron-beam lithography and evaporated directly onto the samples, with wavelengths ranging from 6 to 130 μm. Typically the fundamental, third, and fifth harmonics up to 1.55GHz were observed. At kHz repetition rates, SAW pulses of ~ 0.1 μsec duration were launched across the 2DES mesa, with amplitude and frequency measured using standard boxcar integration and homodyne detection.[4] Sample temperatures down to $\sim$ 50 mK and magnetic fields up to 16T were achieved in a dilution refrigerator/superconducting magnet system.

The principle analysis performed on the data involved comparing the measured d.c. conductivity with the frequency dependent conductivity derived from the SAW measurements. Typical longitudinal d.c. conductivity, SAW amplitude and velocity traces are shown in Figure 1 as a function of magnetic field for relatively low frequency SAW. The dominant features of the sound properties are associated with the IQHE and FQHE.

As shown by the previous work in the IQHE regime,[3] the SAW interaction with the 2D electron layer may be modeled using the d.c. conductivity, $\sigma_{xx}(\omega = 0)$. In this picture,[5-7] the piezoelectric field produced by the SAW interacts with the 2D electron layer and the electron system responds in a manner characterized by a relaxation time represented in the sheet conductivity, σ_{xx} (B). According to this model, the attenuation coefficient Γ

[amplitude$\sim$exp(-Γx)] and the sound velocity v can be calculated from the conductivity using respectively

$$\Gamma = \frac{k(\alpha^2/2)(\sigma_{xx}/\sigma_m)}{1 + (\sigma_{xx}/\sigma_m)^2}$$

and

$$\frac{\Delta v}{v} = \frac{v(\sigma_{xx}) - v_o}{v_o} = \frac{\alpha^2/2}{1 + (\sigma_{xx}/\sigma_m)^2}$$

where α is the effective piezoelectric coupling coefficient[8], $\alpha^2/2 = 3.2\text{x}10^{-4}$, $\sigma_m = v\times(\epsilon_o + \epsilon_s)$ and ϵ_o, ϵ_s are the dielectric constants of the vacuum and semiconductor. Conversely, the 2DES conductivity at the SAW frequency can be extracted using the measured SAW Γ and $\Delta v/v$. Plotted in Figure 1 are fits of the above formulas to the data using the measured d.c. conductivity σ_{xx} and adjusting the parameter $\sigma_m = 4 \times 10^{-7}(\Omega/\Box)^{-1}$ which is reasonably close to the theoretical value. The agreement between the measured sound features and the model results is generally good at low frequencies (<500MHz). This can be interpreted as meaning that at low ω the 2DES conductivity is not substantially different from the d.c. conductivity.

However, at higher frequencies, in particular at $\omega/2\pi>1$GHz, discrepancies arise at FQHE and IQHE states between the d.c. transport and the SAW measurements. At our highest SAW frequencies (1.33 and 1.55GHz) the high order FQHE states are smaller in SAW properties than predicted by the d.c. transport. In addition, FQHE and IQHE states display additional structure or splitting in the SAW velocity. This is most notable at ν=1 and ν=1/3 as seen in Figure 2. These effects are not immediatley attributable to simple 2DES heating. Recent data also show that at the highest frequencies, spin gap filling factors (ν=1,3,5,etc.) have reduced SAW responses in both amplitude and frequency which are not reflected in the d.c. transport. All these findings pertaining to the IQHE and FQHE are preliminary and demand further examination at higher frequencies. To summarize SAW experiments at FQHE and IQHE states, generally good consistency between d.c. and SAW frequency conductivity is observed up to about 500MHz, above which discrepancies occur that remain to be fully tested. The following sections describe unambiguous differences between d.c. and high frequency conductivity occurring at even denominator ν and at $\nu<1/5$.

ν=1/2

The first focus of our study is the pronounced feature at $\nu = 1/2$ in the sound measurements. Figure 2 shows transport and ultrasound data in a magnetic field range centered around filling factor one-half, with FQHE states marked. As expected, when the conductivity drops in the FQHE states, the sound velocity and amplitude increase. Correspondingly, over the broad minimum in σ_{xx} around $\nu = 1/2$, the sound properties increase except immediately near $\nu = 1/2$. Here, the sound velocity and amplitude show a distinct feature with a sharp minimum, in contrast to the broad *maximum* predicted by the conductivity as marked in the Figure. Regardless of the d.c. conductivity model, given the SAW results at integer and fractional ν it is surprising that such a striking feature should appear at filling factor 1/2. The magnitude of this effect is clearly as large as the sound response to several of the higher order fractions (2/5, etc.). The width of the feature is about 4 kG and appears in both frequency and amplitude roughly as an inverted Lorentzian.

The temperature dependence of the strength of the minimum at $\nu = 1/2$ in sound velocity is shown in Figure 3 for the two SAW harmonics in one sample. In the figure the

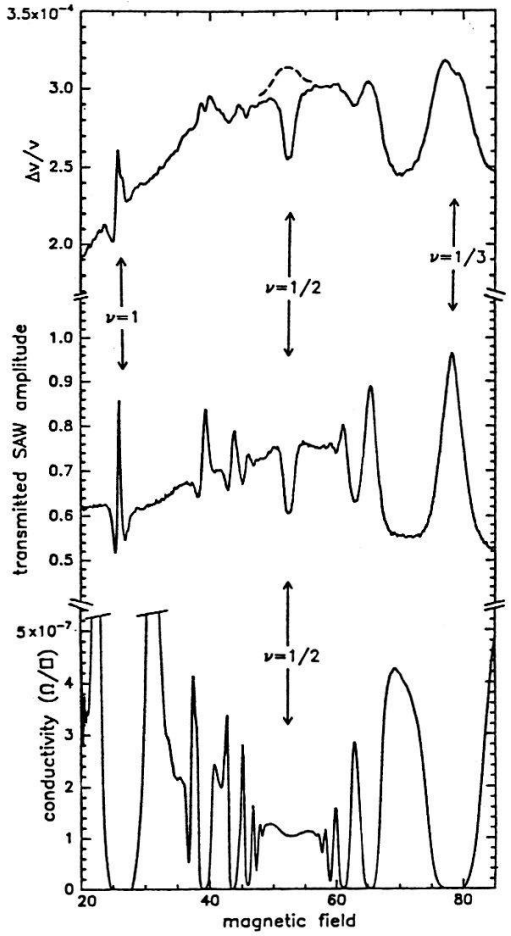

Figure 2. Conductivity, SAW amplitude and velocity shift at 1550 MHz and 50 mK over a magnetic field range centered around filling factor $\nu = 1/2$. The solid lines are measured values and the dashed segments are conductivity model results as in Figure 1 using $\sigma_m = 4.0 \times 10^{-7}\Omega^{-1}$ and slightly offset from the measured trace for clarity. Sample # 1.

depth of the minimum at 1/2 is plotted versus temperature. It is seen that the higher frequency SAW measurements demonstrate stronger anomalies at $\nu = 1/2$ which persist to higher temperatures.

Using the relaxation model, the conductivity deduced from the SAW measurement can be compared to the d.c. measurement. Figure 4 shows measured SAW conductivity and d.c. conductivity as a function of temperature. Over the tested temperature range the SAW derived conductivity increases linearly with decreasing temperature while the d.c. conductivity also increases to a far lesser degree and in a non-linear fashion.

From the data examined so far, the state at 1/2 is unlike the FQHE in $\sigma(\omega)$. However, other tests demonstrate the two to be qualitatively very similar. All ten samples tested displayed the sound anomaly at $\nu = 1/2$, with the strength of the 1/2 state correlated to the appearance of high order fractional states, which in turn reflects high mobility. The temperature range over which the 1/3 FQH state and 1/2 state appear are similar, up to about 1.5K. In previously presented work[9], the 1/2 state was shown to have an electron density dependence similar to the FQHE in that higher densities displayed stronger features at 1/2. These conditions of low temperatures, high mobilities and increased effect with higher electron density strongly suggest a correlation effect, as demonstrated in the FQHE.

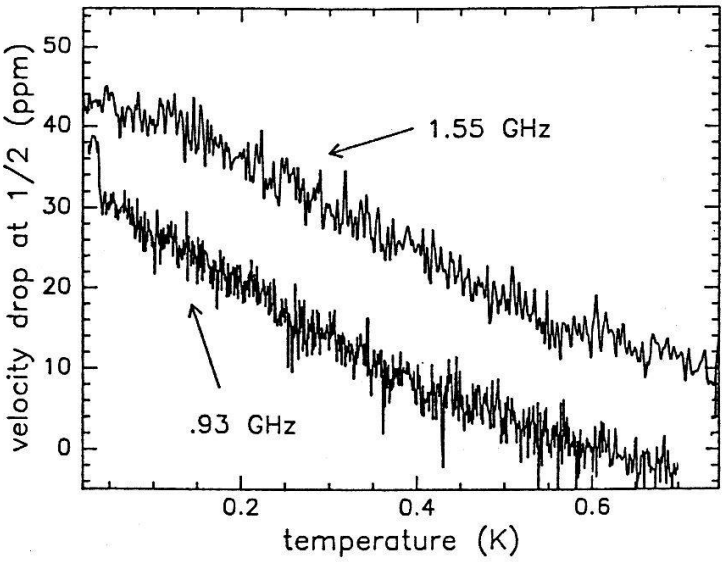

Figure 3. Magnitude of SAW finding at 1/2 for two different frequencies versus temperature. The magnitude is defined as the depth of the amplitude-velocity drop measured against the background near 1/2.

One of the most important pieces of evidence as to the nature of the state at 1/2 is displayed in Figure 5. This data shows that a series of states are exposed by examining the high frequency conductivity. In the figure at low magnetic fields one sees at ν=3/2 a drop in SAW velocity similar to that observed at 1/2 but appropriately extending over a smaller field range. The state at 1/2 is shown for comparison. Remarkably, at ν=1/4 the SAW velocity (and amplitude-not shown here) also demonstrate local minima inconsistant with the d.c. conductivity. The magnetic field extent of the feature at 1/4 is as expected from the states at 1/2 and 3/2. Further study at 3/4 has not definitely displayed these properties. This multiple of states at even denominators, particularly at 1/4, is significant for its analogy to the FQHE. Both in the quantitative conditions for existence and the multiple filling factors, the SAW derived high frequency conductivity states at even denominators are empirically closely related to the FQHE.

The cause of the anomaly at even denominator ν is presently not known. To explore the sources of the sound anomaly one must consider several alternative explanations. First, recent localization studies[10] indicate that the magnetic field range of the extended states at $\nu = 1/2$ obeys $\Delta B \sim T^{\kappa}$ where κ=0.42. Experimentally it is observed that the magnetic field extent of the anomaly does not change appreciably with over an order of magnitude increase in the temperature. In addition, a simple localization picture cannot explain the findings at 1/4. Therefore localization effects are probably not responsible for the $\nu = 1/2$ anomaly.

Another possibility at $\nu = 1/2$ is the presence of a distinct collective electron state, possessing a low frequency mode to which the sound couples over our range of ω and k. In this possibility, the energy scale of the condensate is established to be $\sim$1K by the temperature range over which we observe the 1/2 anomaly in Fig. 3. The simplest excitations of a noncondensed 2DEG are plasma oscillations with no applied B field and cyclotron resonances with an applied B field. The SAW frequencies used here are well below both the cyclotron frequency ($\sim 10^{13}$Hz) at ν=1/2 and the short wavelength ($\lambda \sim 1\mu$m) plasma frequencies ($\sim 10^{12}$Hz) of the 2DES. Therefore, any proposed condensed electron state must have both a condensation energy consistent with the 1K scale of the data and a

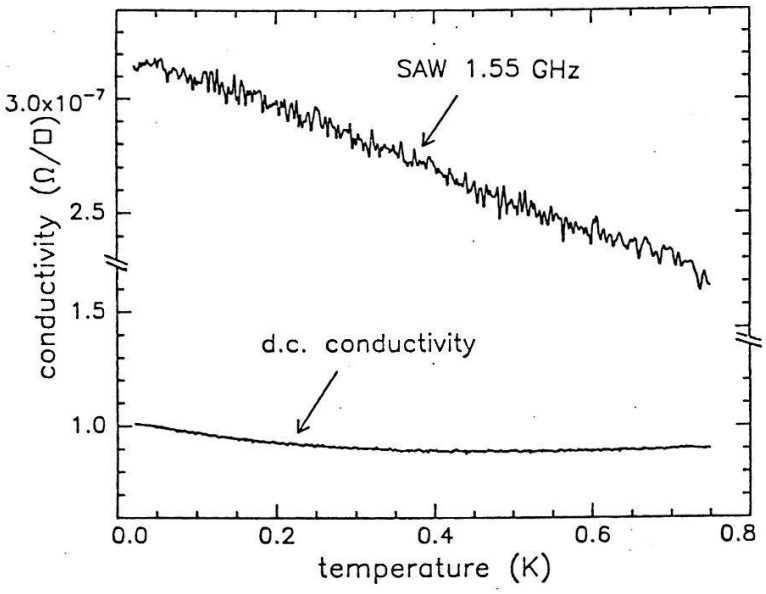

Figure 4. SAW derived conductivity at 1/2 versus temperature and the d.c. measured conductivity.

relatively soft excitation mode in the GHz range to explain the coupling we observe.

A new type of condensed state which is compressible should be considered. Our finding that increased electron density allows observation of the feature to higher temperatures implies that the Coulomb interaction is important. Both increased ultrasound absorption and decreased velocity indicate compressibility. Any speculation upon the nature of such a state must crucially examine the precise filling factor dependence: multiple states at even denominators must be explained. Recent discussions of a paired Hall state[11] at 1/2 deserve scrutiny.

Our favored description of the state at $\nu = 1/2$ giving us these anomalous sound properties is a picture based in the quasiparticle excitation calculations of Halperin[12]. In an iterative formula using pairwise Coulomb interactions of the quasiparticles, quasiparticle-hole potential energies were generated over the filling factor range $0<\nu<1$. In this energy versus ν approximation a marked upward pointing cusp at $\nu = 1/2$ implies instability (negative compressibility), remedied by break up of the 2D electron system into small regions of larger and smaller density. This spontaneous breaking of the translational symmetry lowers the 2D electron system free energy as the resultant electron patches are separately more stable. The energy scale of this picture is roughly correct according to our data; the temperature below which the anomaly is observed in Figures 3 and 4 is $\sim$1K. In Halperin's calculation, to descend from the 1/2 peak to near the ν extent of our 1/2 feature ($\sim$2%), a difference in energy of $\sim$1K is traversed. This lowering of the free energy is balanced by an increase in the Coulomb energy producing clusters or producing a 2DES density fluctuation. If the cluster size is L, one can very crudely model the Coulomb energy of the system as $E_{COUL} \sim e^2(\Delta\nu)^2 nL$ while assessing the free energy gain as $E_{COND} \sim E_0(\Delta\nu)$ where E_0 is the energy/particle[12] at 1/2. The sum of these energy terms can be minimized with respect to a density variation ($\Delta\nu$), as occurs in the phase separation process. This gives us a rough estimate of the cluster size L as $\sim 1\mu$m (excluding consideration of the unknown cluster edge energy). This estimate is consistent with the length scales of our system.

In conclusion, we have observed anomalous SAW propagation at even denominator fillings factors. While FQHE and IQHE states displayed sound amplitude and velocity consistent with d.c. conductivity measurements of the 2DES, at $\nu = 1/2, 3/2,$ and $1/4$ a

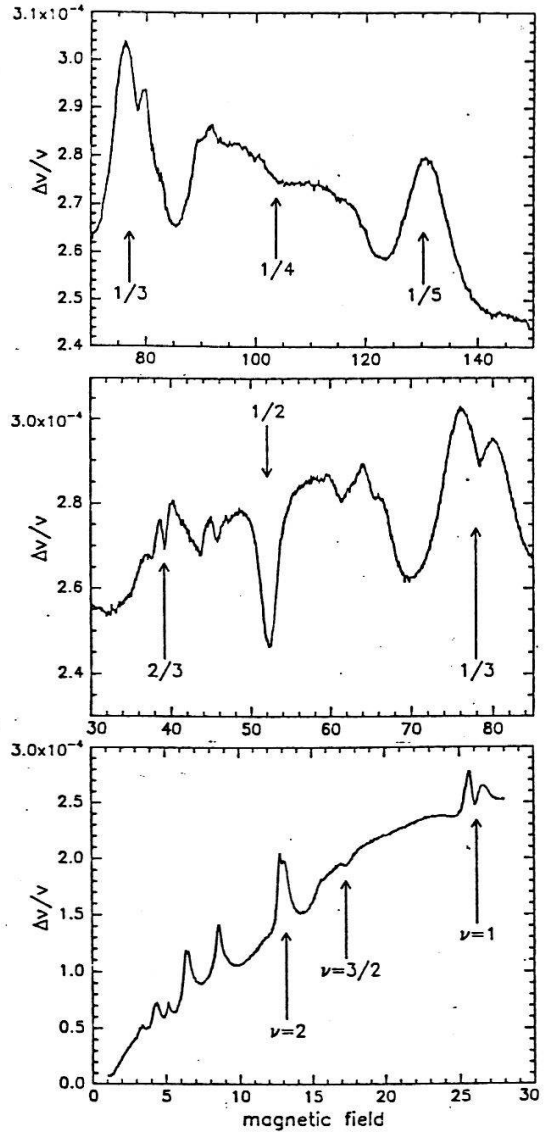

Figure 5. Magnetic field sweeps of SAW velocity at filling factor ranges centered around ν=3/2, 1/2, and 1/4. Note the progressively widening field extent for the even denominator states.

distinctly different response to the SAW field occurs. These features are most pronounced at low temperatures (<100 mK) and high SAW frequencies (>500 MHz). The cause of this effect is yet undetermined, however, it is strongly suggested that spontaneously broken translational symmetry may be the cause. As such these findings represent a study of a process energetically complementary to the FQHE.

$\nu \lesssim 1/5$

The second focus of our studies is the small filling factor range below ν=1/5. It is proposed that in this system of quenched kinetic energy, at sufficiently high B (low ν) the 2DES will condense into an electron solid[2]. The filling factor onset of solidification in the infinite field limit has been predicted[13] to be near ν=1/6. However, in the low density samples we employ this number is expected to be somewhat higher. A large increase in d.c. resistance is expected as solidification occurs, and this effect has been extensively characterized[14].

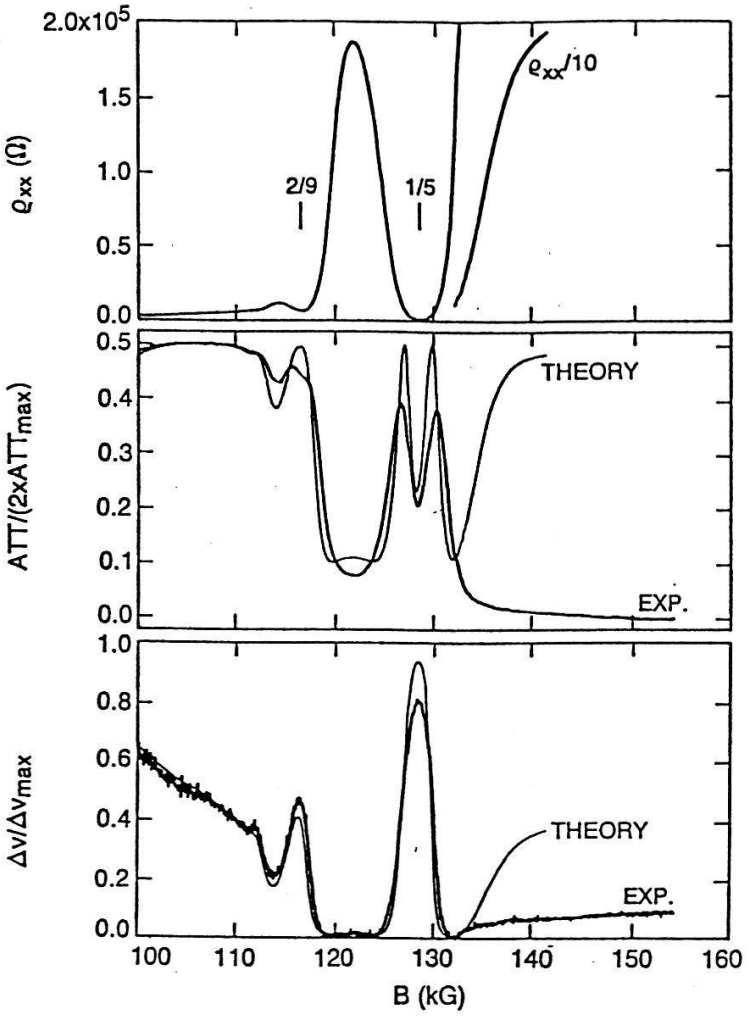

Figure 6. Measured sound velocity shift (solid lines) in the small filling factor range for sample #3 using 235 MHz at three temperatures. The dashed lines are the velocity shift using the measured ρ_{xx} in the d.c. conductivity model.

This property is only a sensitive and not a specific signal of Wigner crystallization; magnetic localization may likewise present as an insulating state in a similar ν range. A specific sign of Wigner lattice formation is propagation of a shear mode with the magneto-phonon dispersion $\omega \sim q^{3/2}/B$. Our sound measurement scheme is designed to detect such a mode. As the magnetic field is varied in the proposed Wigner lattice regime, a crossing of the sound dispersion and magneto-phonon dispersion should appear as an additional absorption channel in the system. The following data represent our investigations into the Wigner lattice filling factor range using the SAW technique.

A prominent discrepancy exists between the ultrasound measurements and the expected sound properties from the d.c. conductivity; see Figure 6. At fields above 1/5 the longitudinal resistivity grows extremely large, and this has been presumed to signal the possible presence of the electron lattice. At these magnetic field values the SAW measurements give much lower sound velocity shift values than expected from the d.c. transport. This suggests that over this range the high frequency conductivity is much larger than the the d.c. conductivity. The raw SAW attentuation results are consistent with this picture; immediately beyond 1/5 the attenuation is small and nearly saturated, as expected for large high frequency conductivity.

In order to understand the SAW results at small ν, we take advantage of the

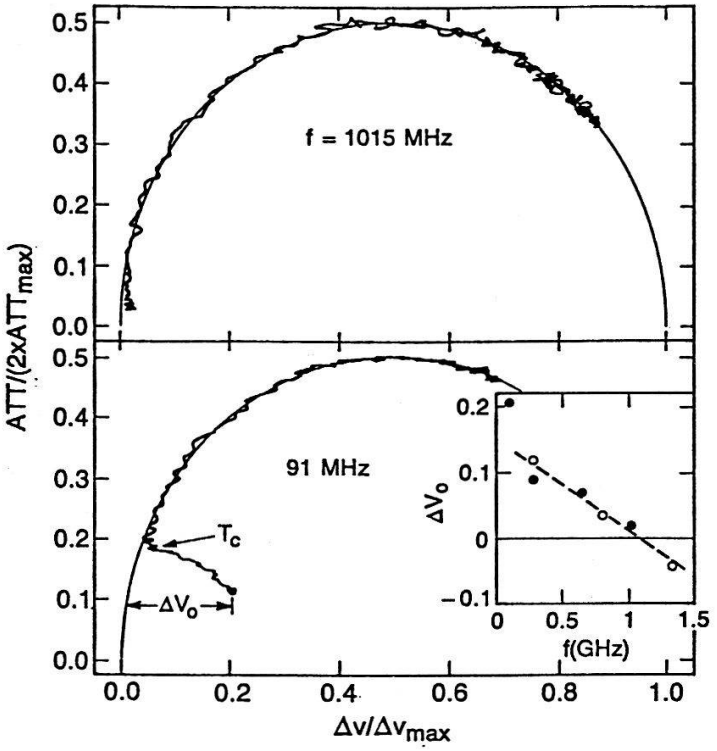

Figure 7. Phase plots of sound attenuation versus velocity shift at two different frequencies for sample #2 at a constant B(ν=0.167). The theoretical line based on Eq.(1) forms a semicircle. In the inset Δv_0 is plotted as a function of frequency for two samples.

measurement of both amplitude and velocity to derive both real and imaginary high frequency conductivity. If an excitation mode is indeed present in the 2DES and the SAW frequency range crosses the mode peak then it is expected that the real part of the conductivity will be peaked at the mode center and the imaginary part of the conductivity will go through zero.

The real and imaginary contributions to the conductivity can be seen immediately in a phase plot of the measured SAW attenuation versus velocity. From equation 1 the phase plot will give a semicircle for only real conductivity and deviations from the semicircle can represent imaginary conductivity. Figure 7 shows phase plots for a high magnetic field point in the presumed electron solid range where the temperature is swept from the highest to lowest values. The highest frequency plot shows data lying on the semicircle or real curve over the entire temperature range with only minor deviation at the low temperature (velocity) end of the sweep. In the low frequency (91MHz) plot at the low temperature end a substantial inward deviation occurs, signalling a sizeable positive imaginary contribution. The deviation initiates at a distinct temperature, T_c. Intermediate frequencies demonstrated intermediate values of Δv_0, the lowest temperature deviation of the SAW velocity from the real conductivity semicircle. These data suggest that as the SAW frequency is increased, at lowest temperature a large imaginary conductivity arises. These values (and others) of Δv_0 are plotted versus frequency in the inset to Figure 7. Δv_0 crosses zero at a frequency of about 1GHz, indicating a mode crossing.

To examine the real part of the conductivity, one can also study temperature sweeps at constant magnetic field values in the insulating regime. Figure 8 shows the conductivity calculated from SAW measurements for two samples with different frequency SAW

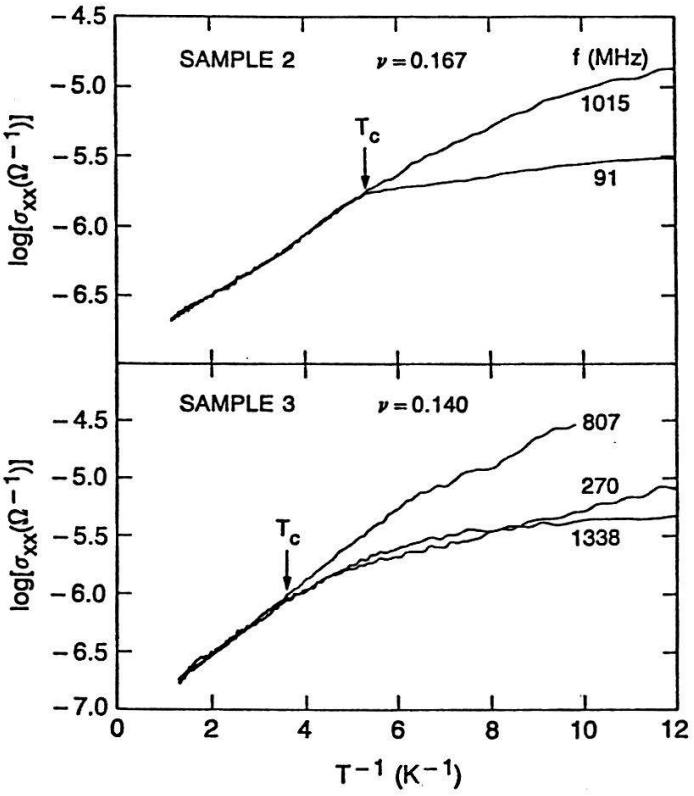

Figure 8. High frequency conductivity $\sigma_{xx}(k,\omega)$ of 2DES in the electron solidification regime as a function of inverse temperature. The insert shows T_c as a function of filling factor ν.

transducers. As the temperature is decreased, different frequency traces have the same conductivity up to a well defined temperature, T_c. At $T<T_c$ the real σ_{xx} behavior is frequency dependent. In sample 2 the higher frequencies have higher conductivity (intermediate ω not shown). In sample 3, one can actually see that at 270 MHz conductivity is less than at 807 MHz which in turn is greater than at 1330 MHz. This indicates that the center of the mode has been crossed. This finding was confirmed in even higher frequency SAW samples up to 1550MHz. Both the real and imaginary conductivities show a mode crossing with a peak near 1 GHz. We interpret the mode observed as a pinning mode of an ordered electron system.

The temperature at which the frequency dependence to the conductivity sets in, Tc, can be mapped out at different filling factors to construct a phase diagram. This is displayed in the Figure 8 inset, and is roughly consistent with the phase diagram expected for electron solidification.

We can estimate the correlation length ξ of the disordered electron solid from the measured pinning frequency. In the long wavelength $k<2\pi/\xi$ regime, the pinning frequency is constant and scales like $\omega_{pl}\omega_t/\omega_c$, where the plasma frequency $\omega_{pl}^2=ne^2k/2\epsilon_p m^*$ and the shear mode frequency $\omega_t^2=\eta k^2/nm^*$ are determined at the wavevector $k=2\pi/\xi$ and the cyclotron frequency $\omega_c=eB/nm^*$. By estimating the shear modulus $\eta=4k_BT_cn$ from the transition temperature $T_c=200$ mK we obtain $\xi=1\mu m$ from our measured pinning frequency at $\nu=.167$. This value of ξ is about 25 lattice spacings of the electron crystal but smaller than our minimum wavelength $\lambda_{min}=2.0\ \mu m$. These findings strongly suggest that the correlation length is no longer than 2 μm.

Additional high frequency conductivity in the small ν range is clearly present and may

well indicate the electron solid formation. In this picture the lower hybrid or shear mode is significantly broadened and the dispersion relation is contorted by the presence of impurities[15]. This results in a broad conductivity peak centered at finite frequencies throughout the small wavevector range. Our data may represent a gradual ascent and crossing of this peak as we increase the SAW frequency. However, the data thus far strongly suggest that if the Wigner lattice is present, disorder is playing a significant role and the system may be better described as a glassy state.

References

[1] D. C. Tsui, H. L. Stormer, and A. C. Gossard, Phys. Rev. Lett. *48*, 1559 (1982).

[2] Y. Lozovik and V. Yudson, Pis'ma Zh. Eksp. Teor. 22, 26(1975) [JETP Lett. 22, 11(1975)].

[3] A. Wixforth, J. P. Kotthaus, G. Weimann, Phys. Rev. Lett. *56*, 2104, (1986).

[4] Sec. e.g. J. Heil, J. Kouroudis, B. Lüthi, and P. Thalmaier, J. Phys. C. *17*, 2433 (1984).

[5] A. R. Hutson, D. L. White, J. Appl. Phys. *33* 40 (1962).

[6] P. Beirbaum, Appl. Phys. Lett. *21*, 595 (1972).

[7] K. A. Ingebrightsen, J. Appl. Phys. *41*, 454 (1970).

[8] T. W. Grudkowski, M. Gilden, Appl. Phys. Lett. *38*, 412 (1981).

[9] H. P. Wei, D. C. Tsui, M. A. Paalanen, A. M. M. Pruisken, Phys. Rev. Lett. *59*, 1776 (1987).

[10] R.L. Willett, M.A. Paalanen "Application of High Magnetic Fields in Semiconductor Physics" Springer-Verlag, 1990- to be published.

[11] M. Greiter, X. Wen, F. Wilczek, Phys. Rev. Lett. *66*, 3205(1991).

[12] B. I. Halperin, Phys. Rev. Lett, *52*, 1583 (1984).

[13] P. K. Lam and S. M. Girvin, Phys. Rev. B30, 473 (1984).

[14] R. L. Willett, H. L. Stormer, D. C. Tsui, L. N. Pfeiffer, K. W. West, K. W. West, K. W. Baldwin, Phys. Rev. B38, 7881(1988).

[15] H. Fukuyama and P. A. Lee, Phys. Rev. B18, 6245(1978).